The OGLE Collection of Variable Stars.
Over 75 000 Eclipsing and Ellipsoidal Binary Systems in the Magellanic Clouds[*]

M. G ł o w a c k i[1], I. S o s z y ń s k i[1], A. U d a l s k i[1], M. K. S z y m a ń s k i[1],
J. S k o w r o n[1], D. M. S k o w r o n[1], P. M r ó z[1], P. P i e t r u k o w i c z[1],
R. P o l e s k i[1], S. K o z ł o w s k i[1], P. I w a n e k[1], M. W r o n a[2,1],
K. U l a c z y k[3,1], K. R y b i c k i[4,1], M. G r o m a d z k i[1] M. M r ó z[1]
and M. U r b a n o w i c z[1]

[1] Astronomical Observatory, University of Warsaw, Al. Ujazdowskie 4,
00-478 Warszawa, Poland
[2] Department of Astrophysics and Planetary Science, Villanova University, 800 East
Lancaster Avenue, Villanova, PA 19085, USA
[3] Department of Physics, University of Warwick, Gibbet Hill Road, Coventry,
CV4 7AL, UK
[4] Department of Particle Physics and Astrophysics, Weizmann Institute of Science,
Rehovot 76100, Israel

ABSTRACT

We present an updated collection of eclipsing and ellipsoidal binary systems in the Large and Small Magellanic Clouds (LMC and SMC), as observed by the Optical Gravitational Lensing Experiment (OGLE) survey. The catalog comprises a total of 75 400 binary systems, including 63 252 in the LMC and 12 148 in the SMC. The sample is categorized into 67 971 eclipsing and 7429 ellipsoidal variables. For all stars, we provide *I*-band and *V*-band photometric time series collected between 2010 and 2024 during the fourth phase of the OGLE project (OGLE-IV). We discuss methods used to identify binary systems in the OGLE data and present objects of particular interest, including double periodic variables, transient eclipsing binaries, double eclipsing binaries, and binary systems with pulsating stars. We present a comparative analysis based on the most comprehensive catalogs of variable stars in the Magellanic System, compiled from surveys like Gaia, ASAS-SN, and EROS-2, and included in the International Variable Star Index.

Key words: *binaries: eclipsing, ellipsoidal - Catalogs*

1. Introduction

More than 50% of all stars are part of binary or multiple star systems Sana *et al.* 2012, Duchêne and Kraus 2013). Binaries are a crucial source of data for modern astrophysics, as they enable direct measurement of fundamental stellar parameters, including the masses, radii, surface temperatures, and absolute magnitudes of their components (Andersen 1991). Additionally, detached eclipsing binaries offer the ability to determine intergalactic distances with better than 1% accuracy (Pietrzyński *et al.* 2019) and provide a unique opportunity to carry out stringent tests of our understanding of stellar structure and evolution. Photometric variations in binary systems can arise from several mechanisms, including eclipses, tidal ellipsoidal distortions, reflection effects, beaming effects, and a variety of phenomena occurring in accretion disks.

The bulge and disk of the Milky Way, along with the Magellanic Clouds, provide natural environments for extensive studies of binary systems. The Optical Gravitational Lensing Experiment (OGLE) project published catalogs containing over half a million eclipsing and ellipsoidal binary systems, including more than 450 000 systems in the Galactic bulge (Soszyński *et al.* 2016), over 11 000 in the Galactic disk (Pietrukowicz *et al.* 2013), approximately 40 000 in the Large Magellanic Cloud (LMC), and more than 8000 in the Small Magellanic Cloud – SMC – (Pawlak *et al.* 2016). These numbers can be compared to the catalogs of binary systems released by other large-scale sky surveys: 154 600 objects in the ASAS-SN catalog of variable stars (Christy *et al.* 2023), 34 562 objects in the EROS-2 database (Kim *et al.* 2014), and over two million eclipsing binary candidates published as a part of the Gaia Data Release 3 (Mowlavi *et al.* 2023). Currently, The International Variable Star Index ((Watson *et al.* 2006), VSX), which compiles variable objects from literature, includes more than one million eclipsing and ellipsoidal variables[†].

Catalogs of variable stars are invaluable in many branches of astronomy. Previously released OGLE catalogs of binary systems enabled search for exoplanets as presented by Mróz *et al.* (2023) or search for binary system candidates hosting a black hole or neutron star (Kapusta and Mróz 2023). The collection was used by various authors to, among others, study fundamental stellar parameters and tidal interactions (Çakırlı *et al.* 2023), to train neural networks for automatic classification of variable stars (Szklenár *et al.* 2020), to study the apsidal motion of eccentric binaries (Zasche *et al.* 2020), to analyze double eclipsing systems (Zasche *et al.* 2019) and to study light travel time effect (Zasche *et al.* 2017).

In this paper, we present an updated collection of eclipsing and ellipsoidal binaries in the Magellanic System. The primary motivation for updating the previous edition of the OGLE catalog of binary systems in the Magellanic Clouds (Pawlak *et al.* 2016) is to include newly identified objects and to refine existing classifications.

[†]*https://www.aavso.org/vsx/* accessed 11.12.2024

Several additional years of OGLE observations collected after the publication of the Pawlak *et al.* (2016(catalog allowed us to identify 27 578 new eclipsing and ellipsoidal variables, to reclassify and remove 783 objects from the previous version of the collection, to refine the orbital periods, magnitudes, amplitudes, and other parameters of the systems, and finally to detect long-term changes and secondary periodicities in numerous variables.

2.　Observations and Data Reductions

The photometric data used in this study were collected during the OGLE-IV project, between March 2010 and May 2024, with the 1.3-meter Warsaw telescope at Las Campanas Observatory in Chile (the observatory is operated by the Carnegie Institution for Science). This telescope is equipped with a mosaic camera composed of 32 CCDs, each with 2048 by 4102 pixels, providing a total field of view of 1.4 square degrees. The surveyed area of the Magellanic Clouds region includes 546 OGLE-IV fields, covering roughly 765 square degrees.

Observations were conducted using the Cousins *I*-band and the Johnson *V*-band filters. The vast majority of the data ($\approx 90\%$) were collected using the *I*-band filter with an exposure time of 150 s. The remaining *V*-band observations were secured with the same integration time. The *I*-band magnitude range captured by OGLE-IV extends from 13 mag to 21.5 mag. The number of epochs collected reaches 5808 in the LMC and 2489 in the SMC, with a median number of epochs equal to 879 and 2274 respectively. The minimal number of epochs collected is 14 in both LMC and SMC.

Photometry was carried out using the Difference Image Analysis method (Alard and Lupton 1998, Woźniak *et al.* 2000). Procedure for the calibration to the standard photometric system together with the detailed information on the OGLE-IV instrumental setup and data reduction system have been described by Udalski *et al.* 2015.

3.　Selection and Classification of Binary Systems

Initially, the *I*-band time-series photometry of 70 million point sources observed by OGLE in the LMC and 14 million in the SMC was processed using the FNPEAKS[‡] program to search for periodic variability. The probed frequency space ranged from 0 to 24 cycles per day with a resolution of 10^{-5} cycles per day. Subsequently, two additional period search algorithms were applied to the light curves with the highest signal-to-noise ratios for the initially derived periods: the string-length method (Dworetsky 1983) and the traditional least-squares fitting of a fourth-order Fourier series. The string-length method is particularly well-suited for highly non-sinusoidal light curves, such as those of eclipsing stars with narrow

---

[‡]*http://helas.astro.uni.wroc.pl/deliverables.php?active=fnpeaks&lang=en*

eclipses. In contrast, the Fourier fitting method is more effective at determining periods for light curves that exhibit continuous variations, as observed in contact and semi-detached binaries. Detected frequencies were refined using the TATRY code based on multi-harmonic periodogram (Schwarzenberg-Czerny 1996) within $\pm 10\%$ range.

The next step of our procedure involved the visual inspection of the light curves phase-folded with the identified periods. After excluding previously known variable stars, we focused on light curves with a signal-to-noise ratio of the detected periodicity greater than 4. To maintain the accuracy of the catalog, candidates for new eclipsing and ellipsoidal variables were independently reviewed by two researchers. In this way, more than 20 000 eclipsing and ellipsoidal variables, not included in the previous version of the OGLE collection (Pawlak *et al.* 2016), were identified. This sample was further expanded with several thousand binaries found in the OGLE (Poleski *et al.* 2010, Wrona *et al.* 2022) and external catalogs of variable stars, including VSX (Watson *et al.* 2006), EROS-2 (Kim *et al.* 2014), ASAS-SN (Christy *et al.* 2023), and Gaia DR3 (Mowlavi *et al.* 2023). More details on comparison between catalogs are provided in Section 5.2. Ultimately, the OGLE collection of variable stars was extended by 27 578 previously overlooked binary systems in the Magellanic Clouds.

The photometry of binary systems included in the Pawlak *et al.* (2016) catalog was updated with new OGLE observations, and the orbital periods, magnitudes, amplitudes, and other observational parameters of these variables were re-derived. After visually inspecting these light curves, we decided to remove 783 objects (1.6% of the total sample) from the catalog, as we reclassified them as pulsating stars, spotted variables, or other types of variable stars. Additionally, for approximately 3700 binaries in the Pawlak *et al.* (2016) catalog, we significantly (by more than 1%) modified their orbital periods.

In the final step of the procedure for selecting and classifying binary systems, we divided our sample into candidates for contact and non-contact eclipsing variables, as well as ellipsoidal variables. The latter group includes eccentric ellipsoidal variables (aka heartbeat stars Wrona *et al.* 2022). Since our classification is based solely on the features of light curves, it should be treated with caution.

4. Binary Systems in the Magellanic Clouds

The OGLE collection of binary systems in the Magellanic Clouds consists of 75 400 objects (63 252 in the LMC and 12 148 in the SMC), of which 67 971 are eclipsing stars and 7421 are ellipsoidal variables. The data for all objects can be accessed through the OGLE web interface or FTP sites:

https://ogle.astrouw.edu.pl → OGLE Collection of Variable Stars
https://www.astrouw.edu.pl/ogle/ogle4/OCVS/lmc/ecl/
https://www.astrouw.edu.pl/ogle/ogle4/OCVS/smc/ecl/

The identifiers of eclipsing binaries follow the convention established in the catalogs of Graczyk *et al.* (2011) and Pawlak *et al.* (2016). Each variable is labeled using the format OGLE-LMC-ECL-NNNNNN or OGLE-SMC-ECL-NNNNNN (where NNNNNN is a six-digit number), based on whether it was located in the sky region covering the LMC or SMC. The boundary between these regions is defined at a celestial meridian of $2^{\mathrm{h}}8$. Ellipsoidal variables in our catalog are designated according to the format OGLE-LMC-ELL-NNNNNN or OGLE-SMC-ELL-NNNNNN.

Observational parameters of all variables, such as equatorial coordinates, orbital periods, out-of-eclipses *I*-band and *V*-band magnitudes, depths of the primary and secondary eclipses, and epochs of the primary eclipse are provided. Depths of the eclipses were measured by finding the baseline and local minima of the light curves smoothed with median filter and Savitzky-Golay filter (Savitzky and Golay 1964). Time series *I*-band and *V*-band photometry obtained during the OGLE-IV survey (2010–2024) is also available. This photometry may be combined with the light curves from previous phases of the OGLE survey (Udalski *et al.* 1998, Wyrzykowski *et al.* 2003, 2004, Graczyk *et al.* 2011, Pawlak *et al.* 2013, 2016), providing three decades long photometric time series, perfect for studying variability in long time scales. However, offsets may occur between the photometric zero points, due to different filters and CCD detectors used during particular stages of the project, as well as due to blending and crowding. Only OGLE-IV light curves were used to determine orbital period and other parameters included in the catalog, unless a given object was observed only during previous surveys. Examples of light curves included in the collection are presented in Fig. 1.

The file remarks.txt contains a list of stars with uncertain classification, along with variables exhibiting atypical properties, *e.g.*, binary systems with a pulsating component, double periodic variables, RS CVn stars, transient eclipsing binaries, etc.

The completeness of our collection of eclipsing and ellipsoidal variables depends on many factors, such as their position in the sky, brightness, amplitude of light variations, period, shapes of their light curves, etc. The highest completeness is expected in the central regions of the LMC and SMC, which have been monitored since 1997 by the OGLE-II and subsequently by the OGLE-III and OGLE-IV projects, and searched for eclipsing variables by Udalski *et al.* (1998), Wyrzykowski *et al.* 2003, 2004, Graczyk *et al.* (2011) and Pawlak *et al.* 2013, 2016. Naturally, our sample does not include objects brighter than the saturation level of OGLE photometry ($I \approx 13$ mag) and stars too faint for their variability to be detected and classified ($I \gtrsim 20$ mag).

The formal completeness of the catalog was assessed using eclipsing and ellipsoidal variables found in overlapping regions of adjacent OGLE-IV fields. These stars could be independently detected twice, although, in the final version of our collection each object is represented by only a one entry from the OGLE database,
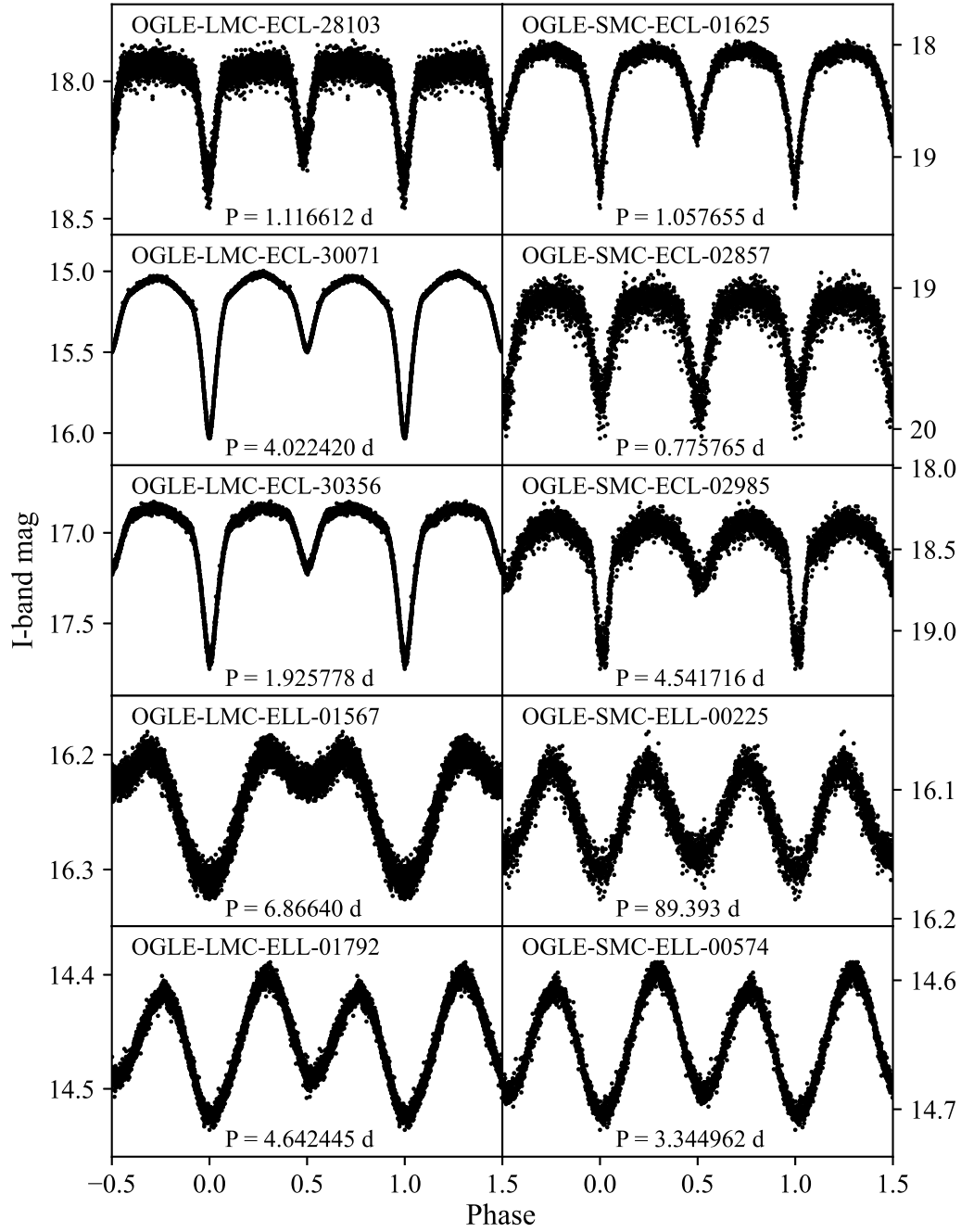
Fig. 1. Examples of light curves of eclipsing and ellipsoidal variables included in this collection. Left column contains objects from the LMC, right one from the SMC. Upper three rows show eclipsing binaries, while bottom two ellipsoidal variables.

typically the one with a light curve containing more data points. Considering only light curves with 50 or more data points, we *a posteriori* found 6018 stars with double identifications in the OGLE-IV database, so we had a chance to find 12 036 counterparts. We independently identified 7886 of them, whereas in 2102 cases, only one component of the pair was identified. Consequently, this leads to the catalog completeness level of approximately 79%. As expected, the faintest stars were the most difficult to identify, along with those exhibiting the smallest amplitudes, detached systems with very long periods, and eclipsing variables displaying additional variability.

5. Discussion

5.1. Catalog Statistics

Simple statistical analysis was performed on the basic parameters of the cataloged objects. Their positions are shown in Fig. 2, which demonstrates that the vast majority of eclipsing and ellipsoidal variables are members of the LMC and SMC. However, some stars lie in the foreground of both galaxies and belong to the Milky Way. Based on the spatial distribution of the objects in the outer fields of the OGLE-IV footprint, we estimate that our collection includes approximately 5000 binary systems from our Galaxy.
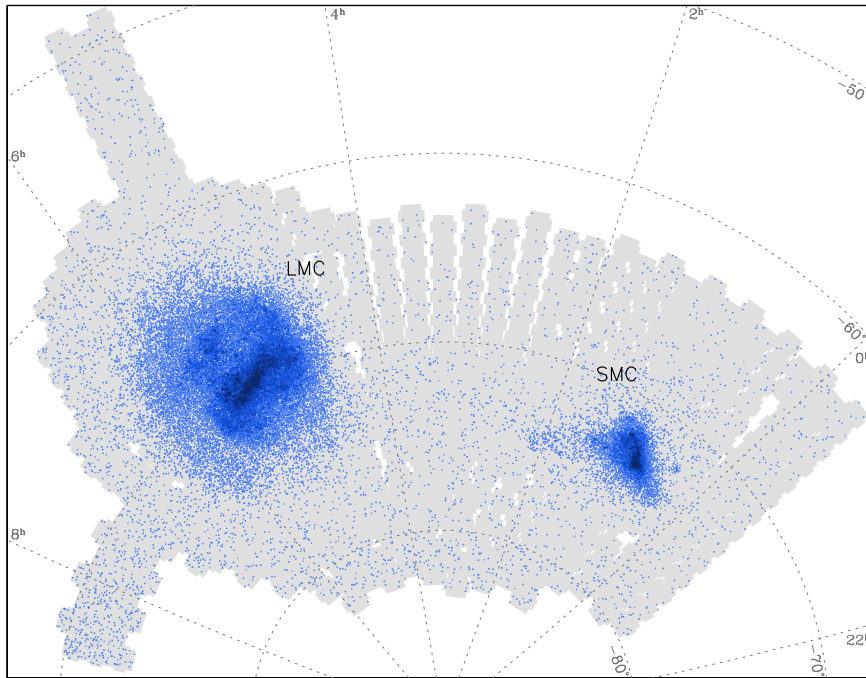
Fig. 2. Spatial distribution of eclipsing and ellipsoidal variables from the OGLE catalog located in the Magellanic Clouds. Darker color of the points indicates higher density of stars in given region. Light gray color in the background represents OGLE-IV fields in the Magellanic System.
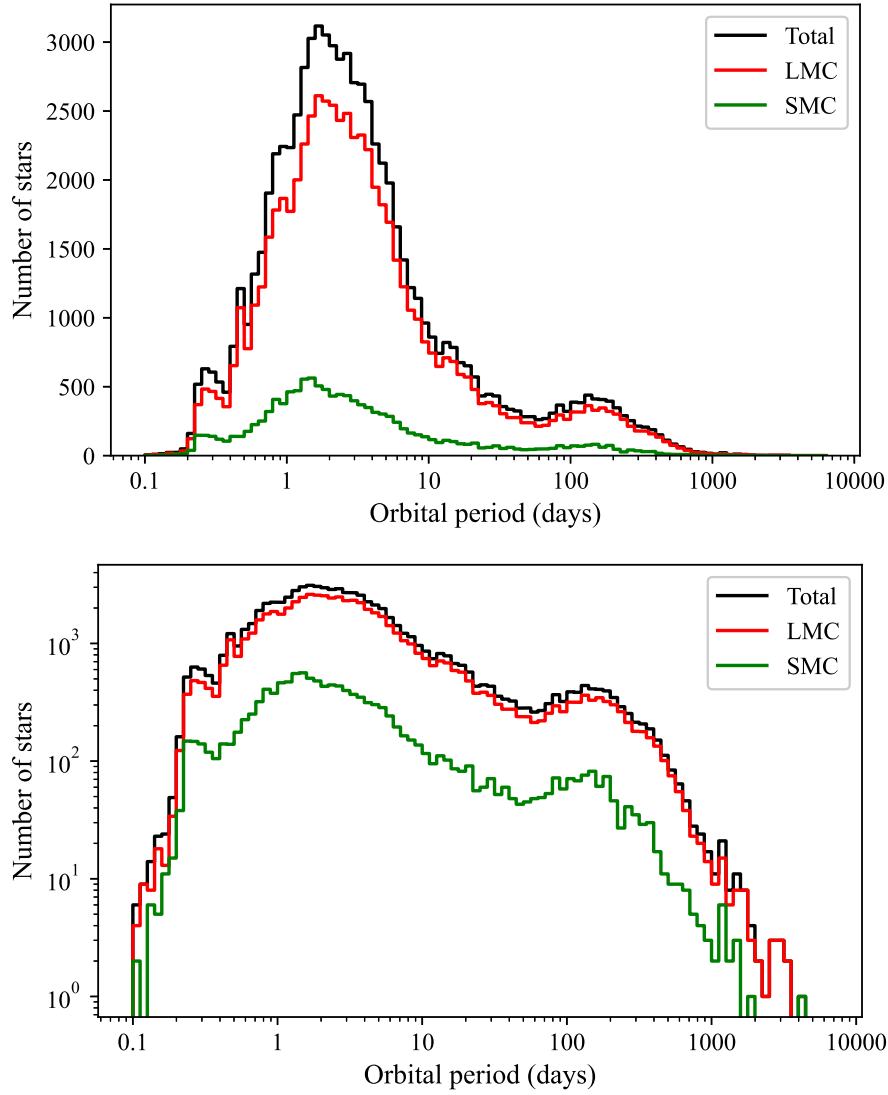
Fig. 3. Distribution of orbital periods of eclipsing and ellipsoidal variables in the Magellanic Clouds. The number of stars is presented in the linear (*upper panel*) and logarithmic scale (*lower panel*). The red, green, and black lines represent histograms for binaries in the LMC, SMC, and both Clouds combined, respectively.

Fig. 3 shows the histograms of orbital periods of binary systems in the Magellanic Clouds. Both LMC and SMC binaries follow similar period distributions, which are also consistent with the distribution of periods obtained by Soszyński *et al.* (2016) for eclipsing and ellipsoidal binaries in the Galactic bulge. In particular, the period distributions of binary systems in both the Magellanic Clouds and the Milky Way exhibit a local maximum for periods between 100 d and 200 d, which is mainly caused by close systems (usually ellipsoidal variables) consisting

of red giant stars. In contrast, the main peak of the period distribution for binaries in the Magellanic System occurs at around 2 d, which does not align with the maximum at 0.4 d for stars observed toward the Galactic bulge (Soszyński *et al.* 2016). This discrepancy arises from a selection effect: most short-period contact systems (W UMa stars) in the Magellanic Clouds are too faint to be detected with the 1.3-meter OGLE telescope. Indeed, objects classified as contact binary systems constitute only 4% of our sample of eclipsing variables in the Magellanic Clouds (a significant portion of them lies in front of the Magellanic Clouds and belongs to the Milky Way halo), whereas in the Galactic bulge, more than 20% of all eclipsing stars are W UMa-type systems.

The distribution of out-of-eclipse *I*-band magnitudes of our variables is shown in Fig. 4. The shape of this distribution reflects both the luminosity function of binary stars in the Magellanic Clouds and the detection limits for variable stars using OGLE photometry. The histogram has a maximum around $I = 19.5$ mag. For fainter stars, the completeness of our catalog declines sharply. Additionally, the LMC distribution has another maximum at around 16 mag, most probably due to a high population of luminous stars from the tip of the red-giant branch.

All LMC and SMC objects were presented in a color-magnitude diagram (Fig. 5, after correcting their $V - I$ color index and *I*-band magnitude for extinction using reddening maps created by Skowron *et al.* (2021). The diagram shows that roughly 75% of the stars in our catalog lie on the main sequence, while the majority of the remaining systems contain red giant stars.
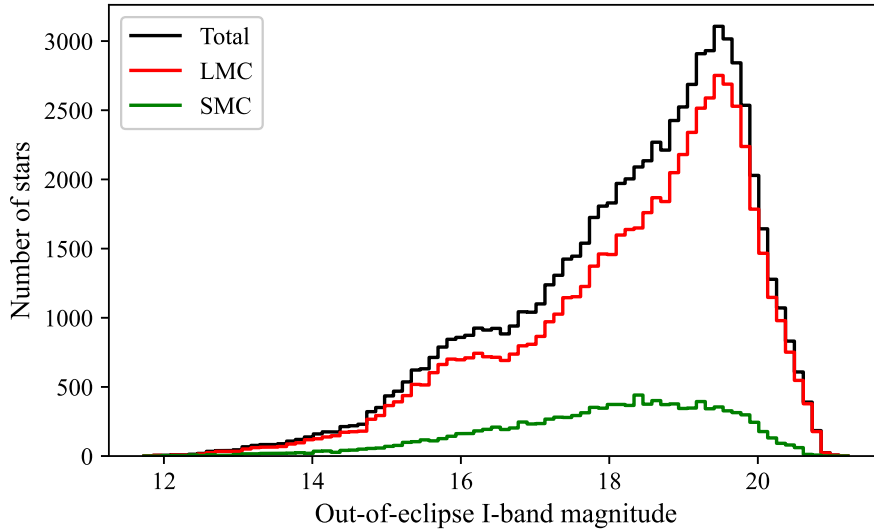

Fig. 4. Distribution of out-of-eclipse *I*-band magnitudes of eclipsing and ellipsoidal variables from the OGLE catalog located in the Magellanic Clouds.
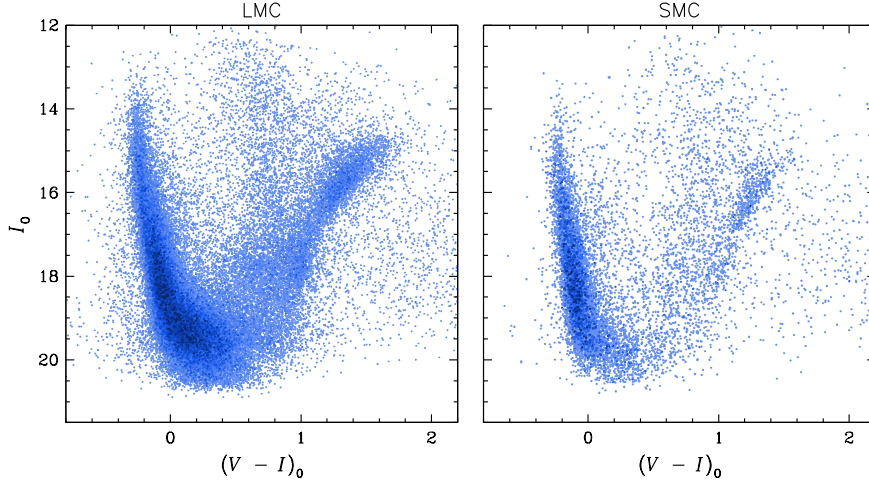
Fig. 5. Color–magnitude diagram for eclipsing and ellipsoidal variables from the OGLE catalog located in the Magellanic Clouds. The color of points indicates the density of stars.

5.2. *Cross-Match with other Catalogs*

As mentioned in Section 3, to enhance the completeness of our collection, we cross-matched point sources observed by OGLE with candidate eclipsing binaries published in the ASAS-SN (Christy *et al.* 2023), VSX (Watson *et al.* 2006), EROS-2 (Kim *et al.* 2014), and Gaia DR3 (Mowlavi *et al.* 2023) catalogs. A careful visual inspection of the OGLE light curves of the stars selected in this way allowed us to increase the size of our collection by approximately 5000 objects.

Some candidates from other catalogs were rejected because of lack of periodic variability in the OGLE data or because the variability did not match with binary systems. The remaining objects were also excluded from the final version of this collection because of too small amplitude, too high brightness, inaccurate coordinates in different catalogs, localization in the area corresponding to the technical gaps between CCDs, etc.

For each external catalog, orbital periods of all matched objects were compared with the main orbital periods from the presented catalog and with their harmonics as follows:

$$P_k = k^{\pm 1} P_{\text{OGLE}} \quad \text{for} \quad k \in \left\{ 1, \frac{3}{2}, 2, 3, 4 \right\} \tag{1}$$

where P_{OGLE} is the orbital period measured from the OGLE light curves and provided in our collection. Fig. 6 compares the orbital periods for ASAS-SN, VSX, EROS-2 and Gaia DR3 respectively. The summary results of the cross-matching with other catalogs are presented in Table 1.

For ASAS-SN and VSX catalogs, almost all objects have orbital periods directly matching with our data. However, the orbital periods provided in the EROS-2 catalog differ significantly from the values measured from the OGLE light curves. Most of them are equal to half the expected values. The discrepancies between the
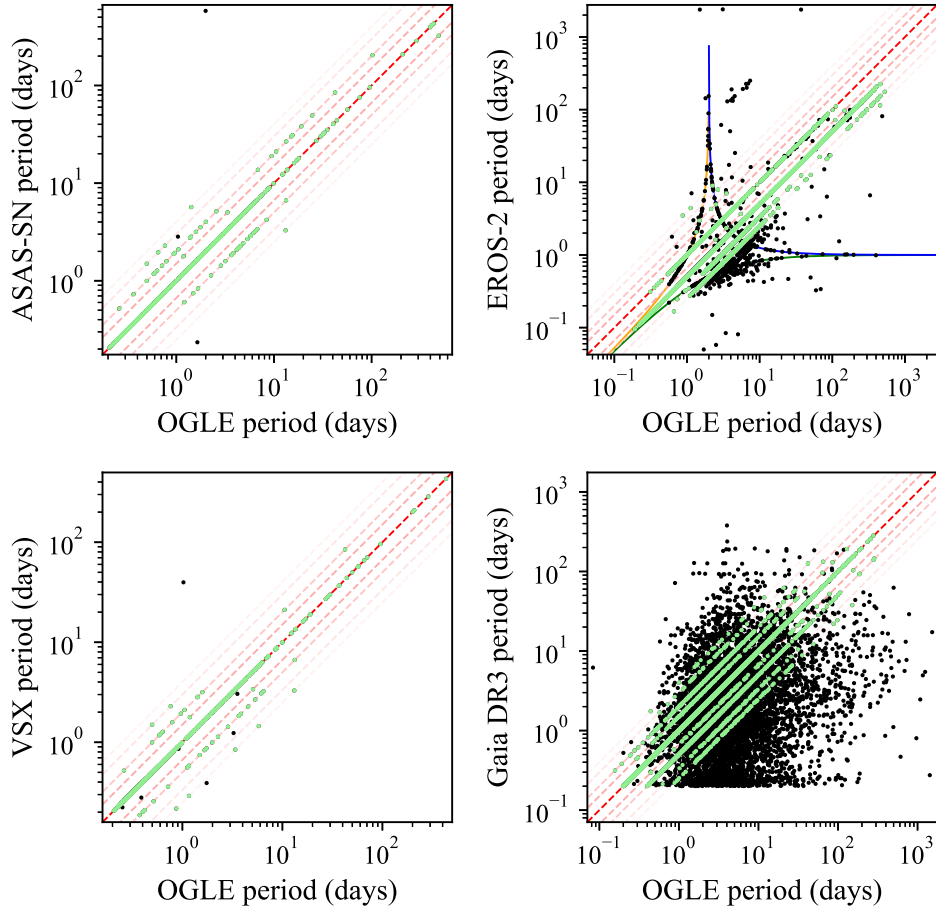
Fig. 6. Comparison of the orbital periods measured with OGLE data with the orbital periods from external catalogs. The red dashed lines represent orbital period harmonics defined in the Eq.(1), with the intensity of the color decreasing for higher values of k. The green points represent objects with matching periods.

T a b l e 1

Comparison of binary stars catalogs

Catalog	ASAS-SN	VSX	EROS-2	*Gaia* DR3
Objects within OGLE fields in the MC	1707	1675	53 942	38 827
Matched with OGLE catalog	65%	62%	43%	61%
Objects misclassified as binaries	7.5%	0.66%	5.4%	0.82%
Objects rejected from the OGLE catalog	5%	10%	50%	35%
Matching period	95%	96%	4.1%	65%
Matching period (with multiples)	99.7%	99.3%	97.3%	75.3%

EROS-2 data and the OGLE data were also described by Poleski (2014). Additionally, the following period aliases are also included in EROS-2 data (see upper right panel in Fig. 6):

$$f_1 = 2f_{\text{OGLE}} + 1 \qquad \text{(dark green line)}$$
$$f_2 = 2f_{\text{OGLE}} - 1 \qquad \text{(orange line)}$$
$$f_3 = -2f_{\text{OGLE}} + 1 \qquad \text{(blue line)}$$

where $f_i = P_i^{-1}$. There is a very significant discrepancy between Gaia DR3 and OGLE orbital periods, which does not follow any regular pattern. This suggests high degree of randomness in orbital periods in Gaia DR3 catalog, which also means that those stars were correctly classified as eclipsing or ellipsoidal variables by coincidence.

5.3. Binaries with other Types of Variability

Among binary stars included in this work, there are interesting groups of objects showing additional variability. The selected groups are described below.

RS Canum Venaticorum (RS CVn) stars are binary objects with darker spots on the surface, introducing additional semi-regular variability between eclipses. The light curves of selected objects are presented in Fig. 7. Our collection contains at least 294 variables of this type.

Transient eclipsing binaries – these objects do not show eclipsing variations at all times. For example, eclipses may gradually appear or disappear, or may occur in cycles. They were first described by Graczyk *et al.* (2011). Analysis of such a long term variability is possible thanks to combined OGLE photometric data from multiple years of observations. Some of the transient eclipsing binaries from this catalog are presented in Fig. 8. When these stars do not show eclipsing variability, they may retain ellipsoidal behavior (Fig. 9), or reflection effect (Fig. 10).

Binary systems with pulsating stars – binary systems where at least one of the components is a pulsating star (*e.g.*, a Cepheid or RR Lyrae star). Fig. 11 contains some of such objects from this collection.

Double eclipsing binaries are objects in which two superimposed eclipsing or ellipsoidal modulations are simultaneously visible. Our collection contains more than 150 such systems. The light curves for selected stars are presented in Fig. 12. Most probably they are quadruple systems consisting of two pairs of eclipsing/ellipsoidal variables orbiting common center of mass.

Systems with apsidal motion – due to a strong apsidal motion, each eclipse for these objects phases with slightly different period. Examples of such objects from this collection are presented in Fig. 13.
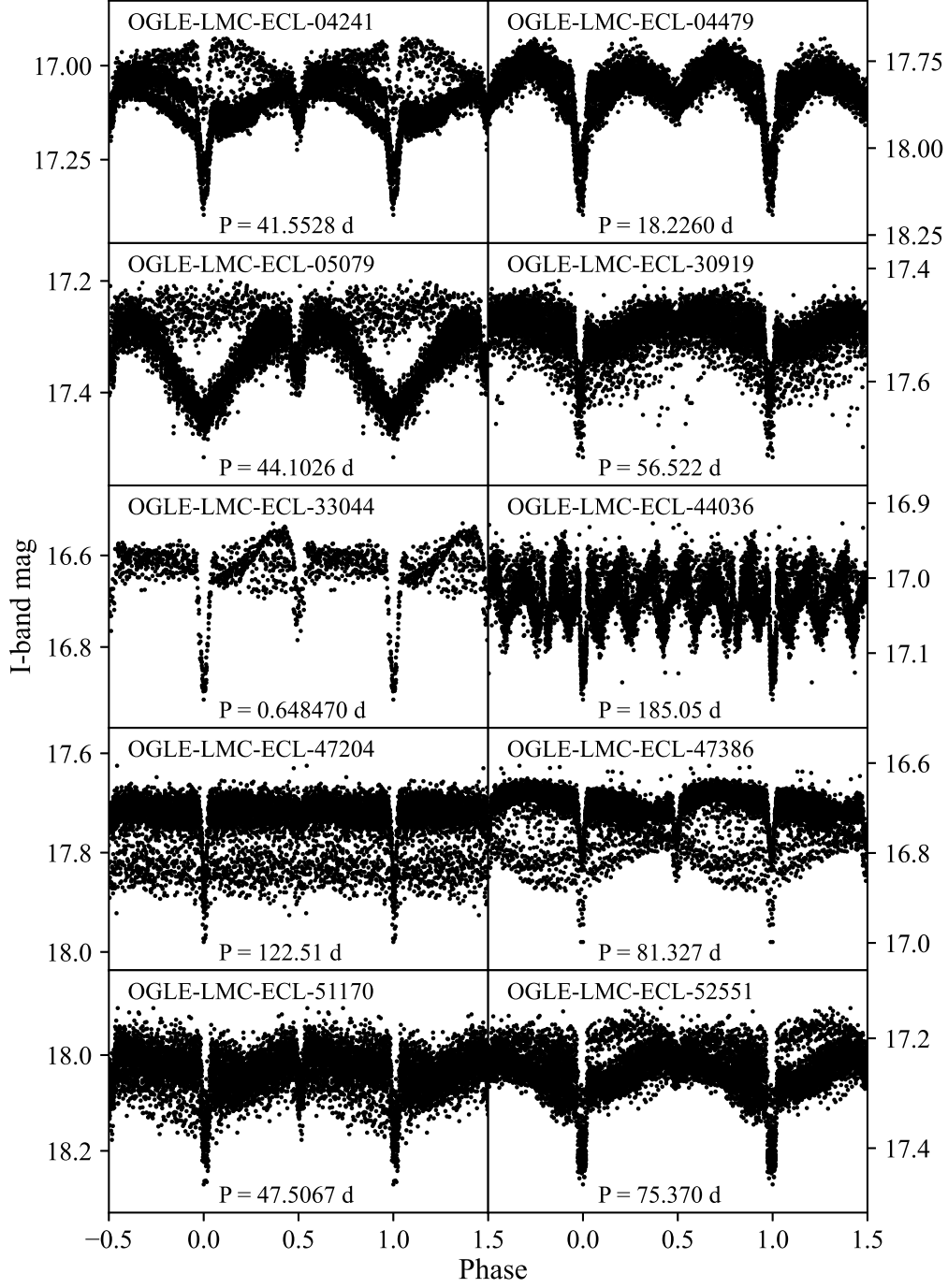
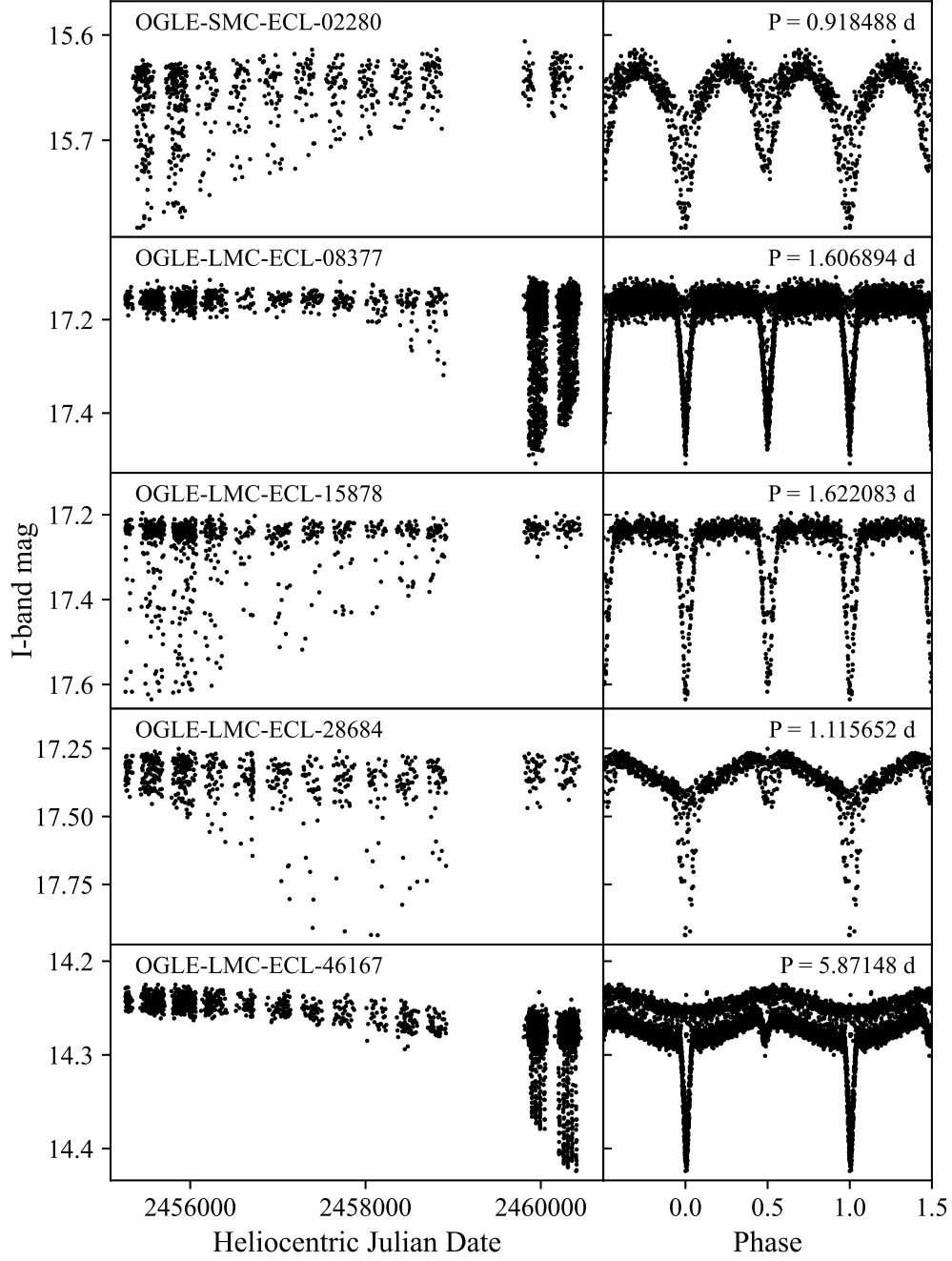Fig. 7. Light curves of selected RS CVn stars folded with the orbital periods.

Fig. 8. Phase-folded light curves of selected transient eclipsing binaries from this work. Each row represents one object, showing both time-domain and phase-folded light curve.
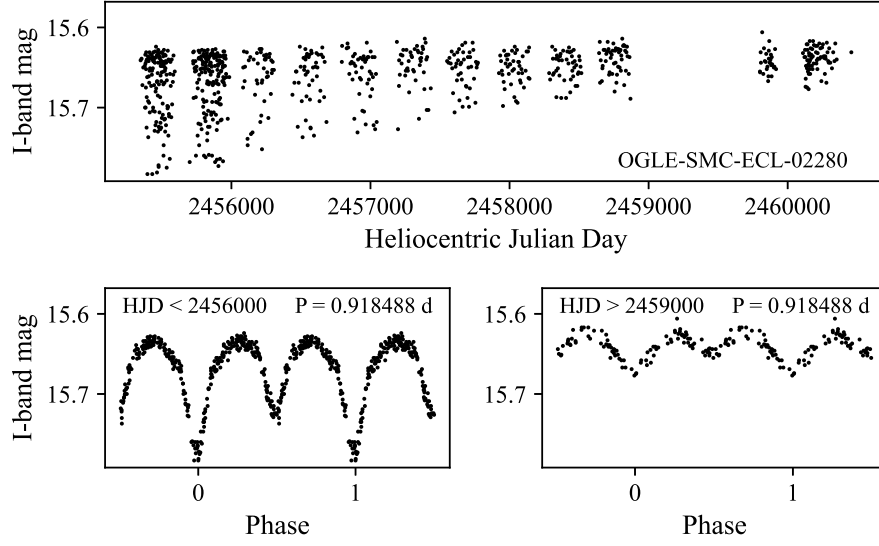
Fig. 9. Transient eclipsing object retaining ellipsoidal variability when eclipsing behavior ceases. *Upper panel* shows unfolded light curve obtained from OGLE-IV data. *Left lower panel* shows phase-folded light curve from first three observational seasons (with visible eclipses), whereas the *right panel* shows the phase-folded data from the last two seasons (with ellipsoidal variability).
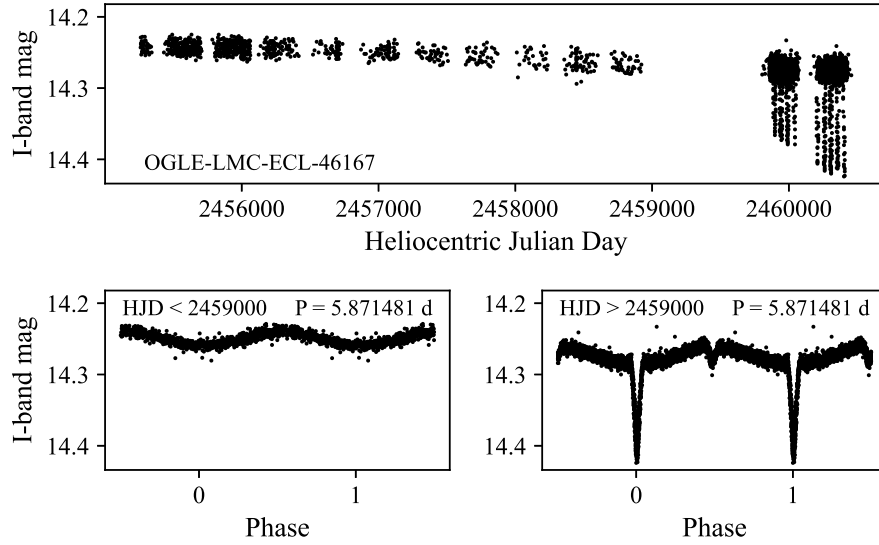
Fig. 10. Transient eclipsing object showing reflection effect with later appearing eclipses. The upper panel shows unfolded light curve obtained from OGLE-IV data. *Left lower panel* was detrended for clarity due to change of average magnitude over time, and shows phase-folded light curve from first 11 observational seasons with visible reflection effect. *Right panel* shows eclipsing behavior of the object in the last two seasons.
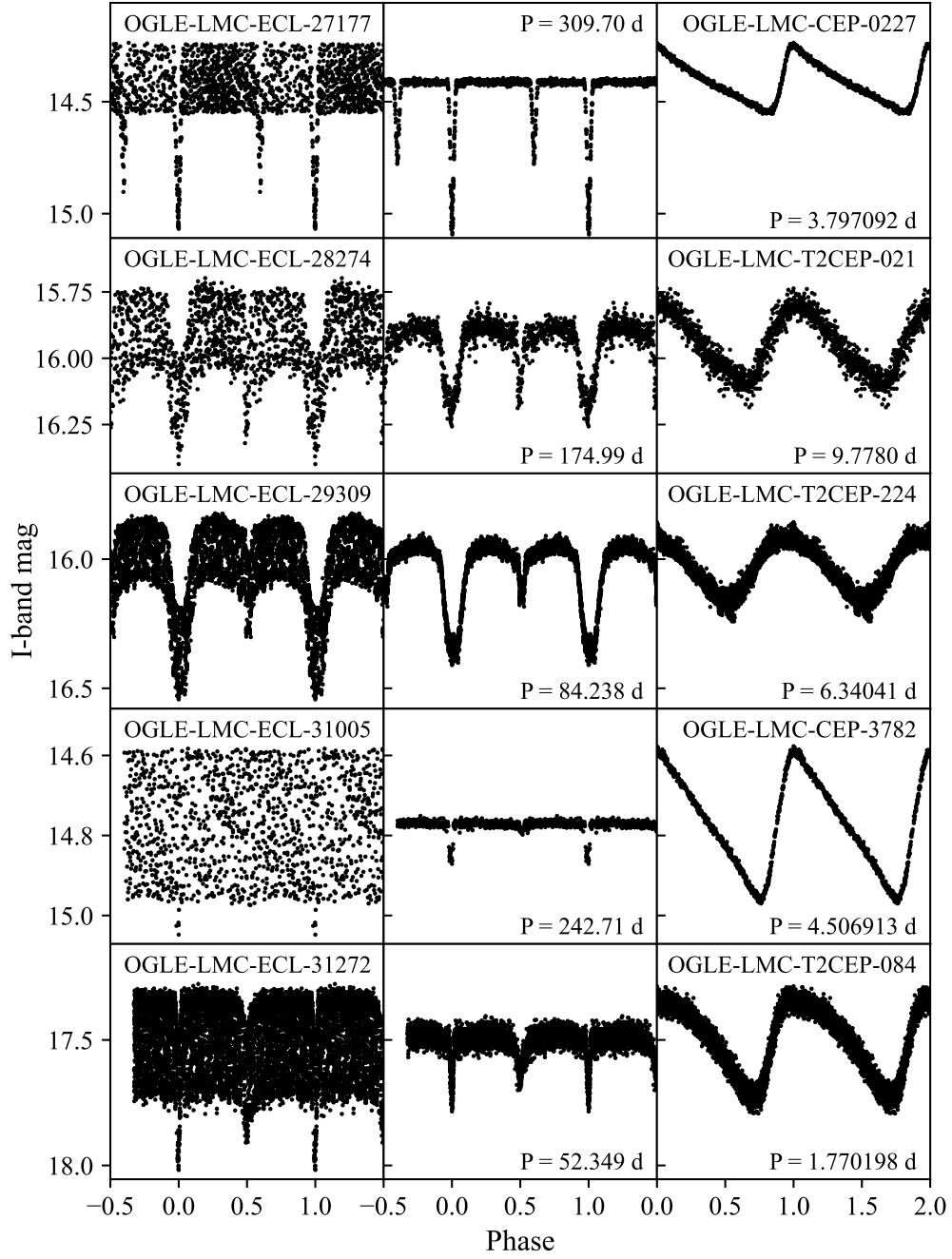
Fig. 11. Light curves of selected systems with pulsating stars from this work. *Left panels* show the original light curves folded with the orbital periods, while *middle* and *right panels* present the disentangled eclipsing and pulsating light curves, respectively.
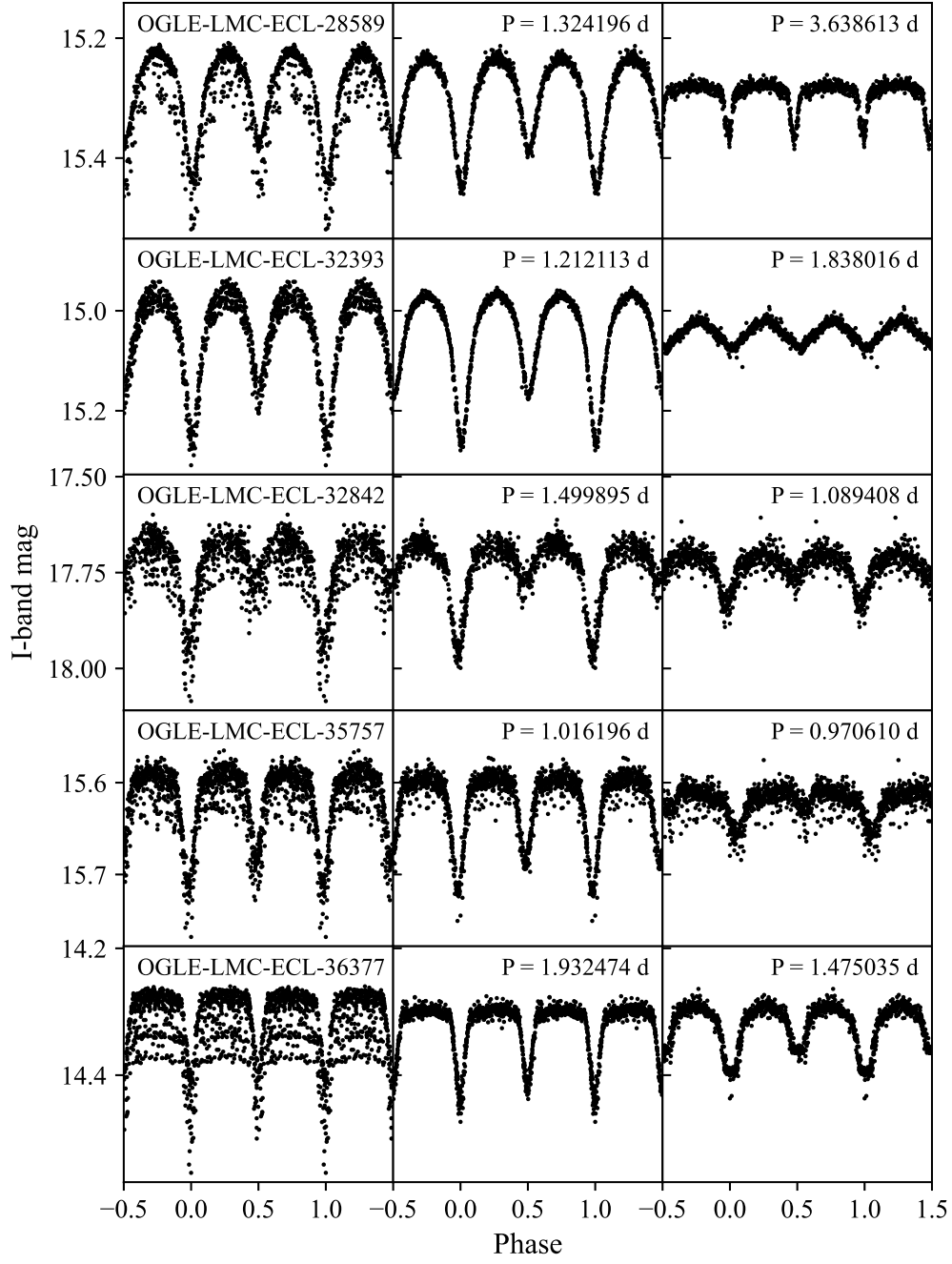
Fig. 12. Light curves of selected double eclipsing systems from this work. *Left panels* display the original light curves folded with one of the orbital periods, while *middle* and *right panels* present the disentangled light curves folded with both orbital periods.
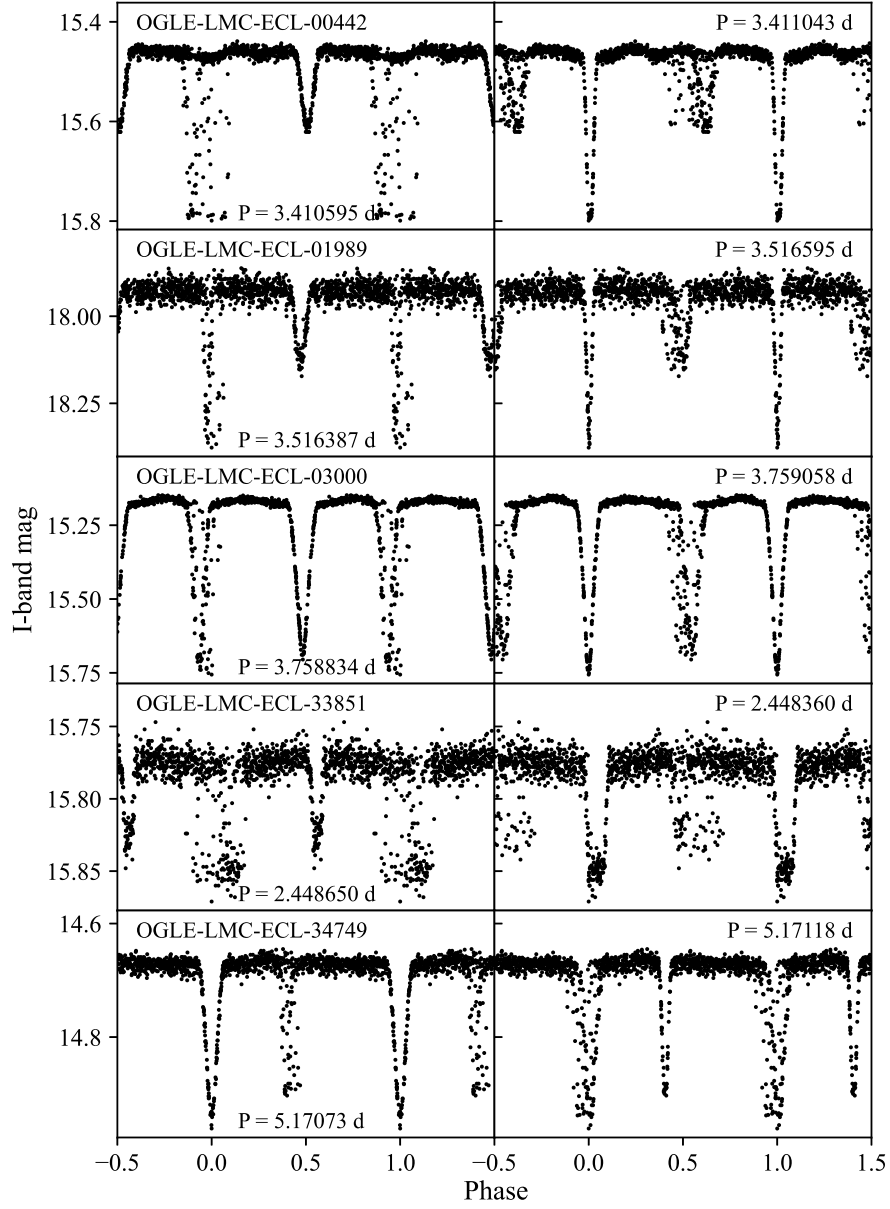
Fig. 13. Phase-folded light curves of selected systems with strong apsidal motion from this work. Each row represents the same object, with light curve phase-folded with slightly different periods.
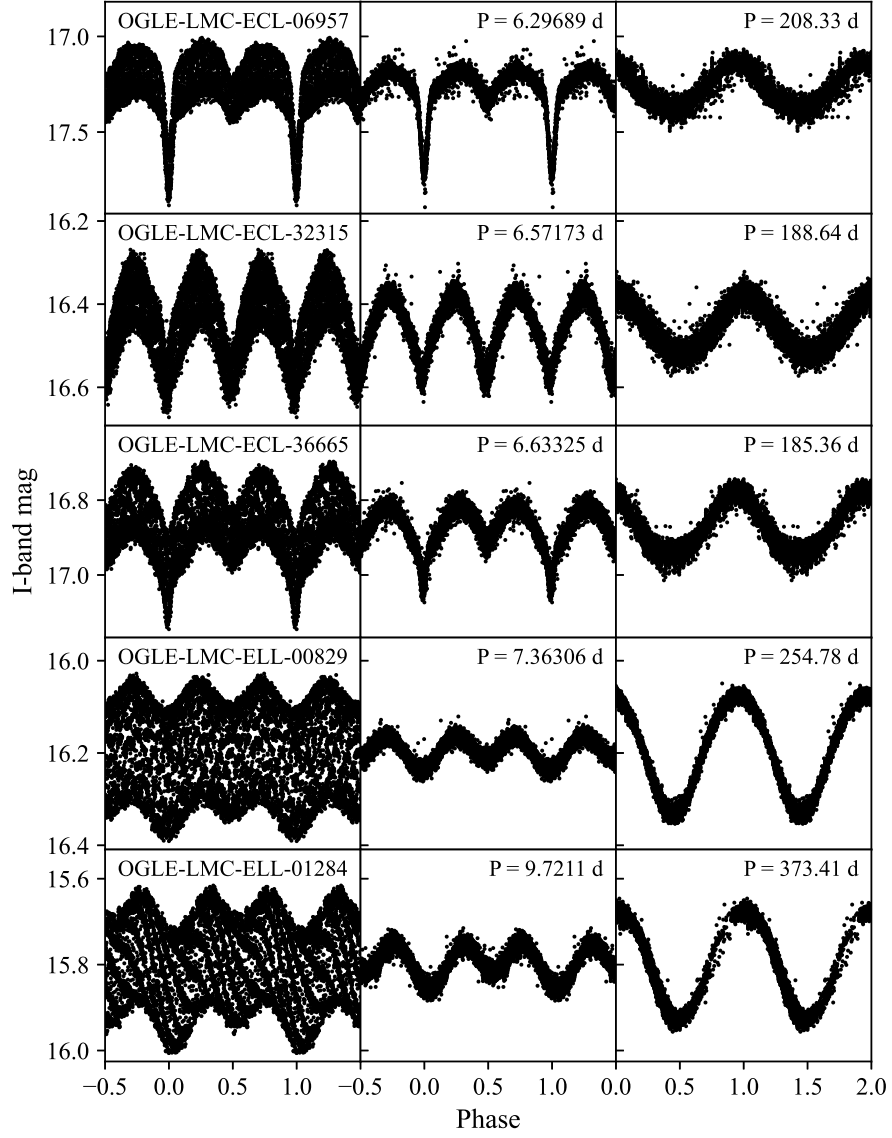
Fig. 14. Light curves of selected DPV stars from this work. *Left panels* show the original light curves folded with the orbital periods, while *middle* and *right panels* present the disentangled eclipsing and long periodic variability light curves, respectively.
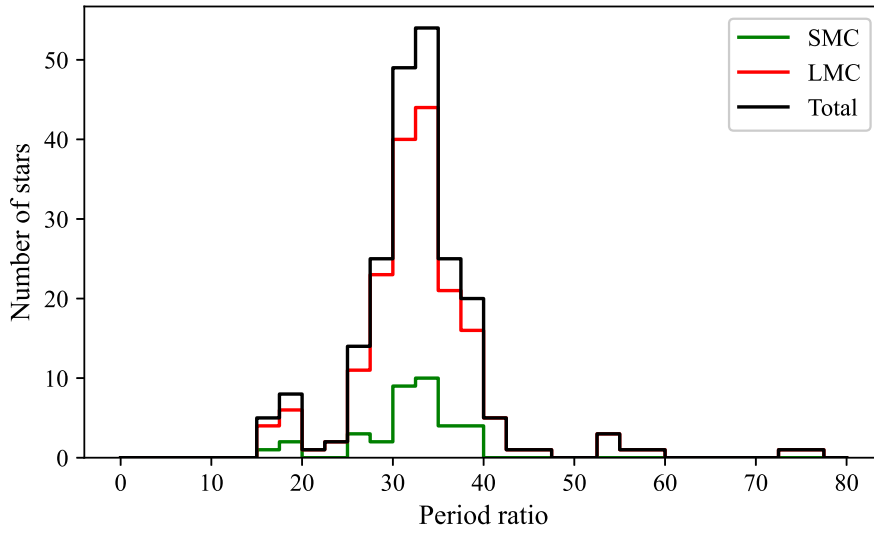
Fig. 15. Distribution of ratios of longer periods to orbital periods for DPV stars included in this catalog.
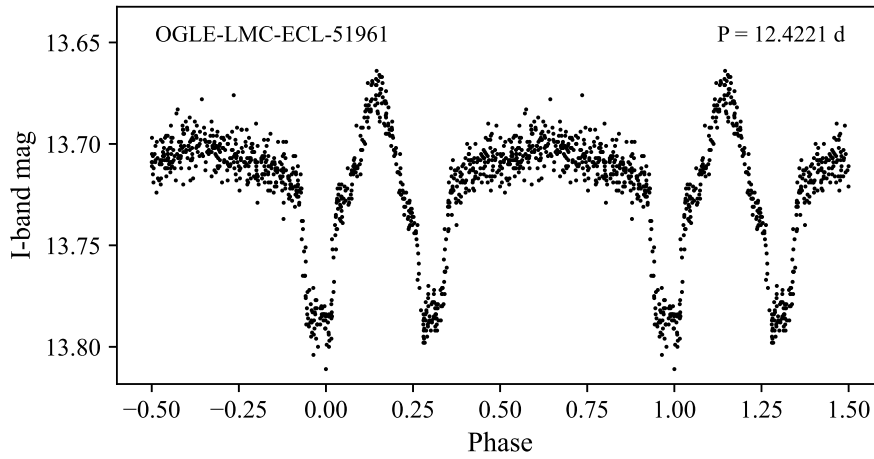

Fig. 16. Phase-folded light curve of a peculiar binary object. The object becomes significantly brighter between eclipses, which separation is also quite low. Most probably it is eccentric ellipsoidal variable with visible eclipses.

Double periodic variables (DPVs) are binary stars with a long secondary period, first recognized by Mennickent *et al.* (2003). Typically, it is around 33 times greater than the orbital period. This catalog contains 220 objects of this type, extending the previous OGLE catalog of DPVs published by Poleski *et al.* (2010) by 95 new objects. The selected objects are presented in Fig. 14. The distribution of the ratios of their longer periods to shorter periods is shown in Fig. 15.
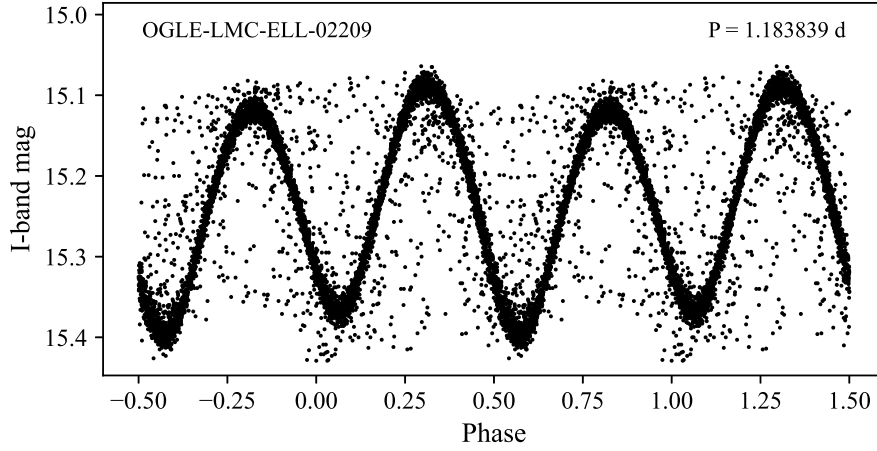
Fig. 17. Phase-folded light curve of ellipsoidal variable with significant changes of orbital period. Its light curve was divided into year-long segments and phase-folded with different orbital periods in Fig. 19.
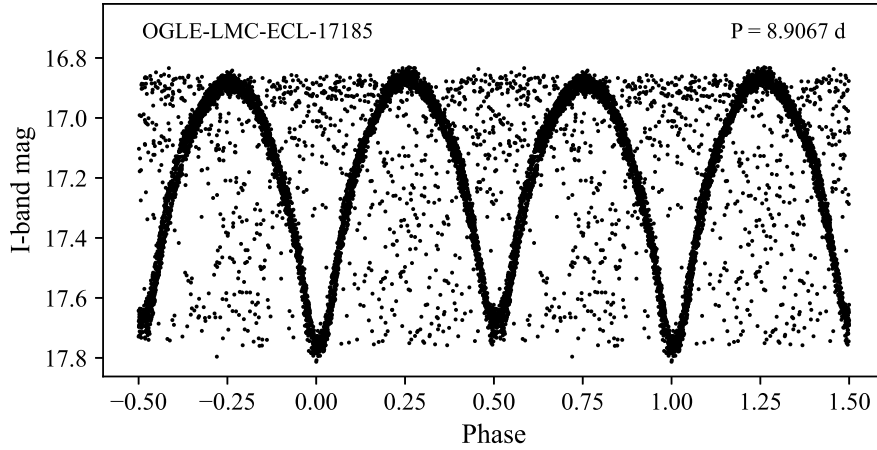

Fig. 18. Phase-folded light curve of eclipsing variable with significant changes of orbital period. Its light curve was divided into year-long segments and phase-folded with different orbital periods in Fig. 20.

Peculiar objects – some objects exhibit additional variability that is difficult to classify and explain, for example, the OGLE-LMC-ECL-51961 object (presented in Fig. 16). Most probably it is an eccentric ellipsoidal variable with $\omega \approx 0°$ or $\omega \approx 180°$ as described in Wrona *et al.* (2022), with visible eclipses. Other examples of interesting objects are OGLE-LMC-ELL-02209 and OGLE-LMC-ECL-17185 (presented in Figs. 17 and 18 respectively) showing significant decrease in orbital period over time. Their light curves were divided into year-long segments, and each segment was phase-folded with manually adjusted orbital period (Figs. 19
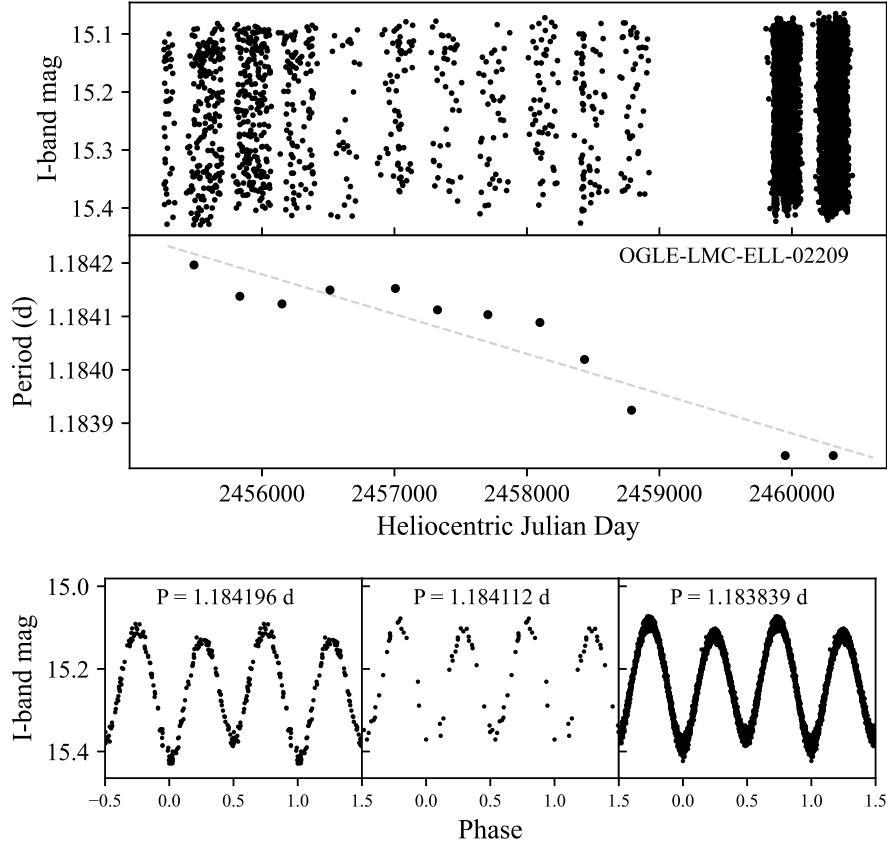
Fig. 19. *Upper panel* shows the light curve and manually adjusted orbital period for year-long frag-
ments. The gray dashed line represents the fitted linear function, used to determine the rate of period
change: 2.72×10^{-5} d/yr. *Lower panel* shows pieces of this light curve phase-folded from the first
season, season in the middle, and the last season with manually adjusted periods. Despite changes of
the orbital period, the shape of the light curve remains unchanged.

and 20). The linear function was fitted to determine the average rate of period
changes: 2.72×10^{-5} d/yr and 2.01×10^{-3} d/yr respectively. The latter object
also started exhibiting the O'Connell effect in the last observational season. Anal-
ogous behavior was observed in the red nova V1309 Scorpii progenitor before its
outburst (Tylenda *et al.* 2011), with an average period decrease of 3.46×10^{-3} d/yr
and similar changes in the shape of the phase-folded light curve.

6. Conclusions

We presented the OGLE collection of eclipsing and ellipsoidal variables in the
Magellanic Clouds. The new catalog contains over 50% more objects than the one
previously published by Pawlak *et al.* (2016), and it is the largest catalog of such
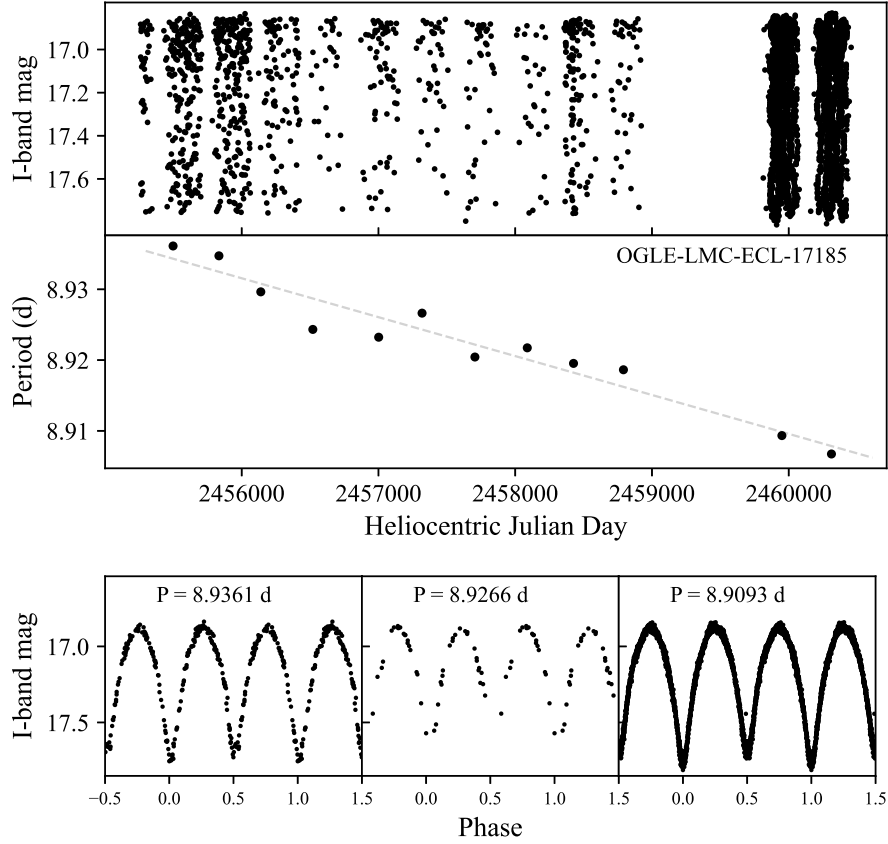binary systems in the Magellanic Clouds up to date. For each object we provide

Fig. 20. *Upper panel* shows the light curve and manually adjusted orbital period for year-long fragments. The gray dashed line represents the fitted linear function, used to determine the rate of period change: 2.01×10^{-3} d/yr^{-1}. *Lower panel* shows pieces of this light curve phase-folded from the first season, season in the middle, and the last season with manually adjusted periods. In the last observational period the object started exhibiting the O'Connell effect.

orbital period, depth of eclipses, out-of-eclipse magnitude, color, and long time-series *I*-band and *V*-band photometry.

Our collection contains unusual objects of particular interest: double periodic variables, transient eclipsing binaries, binaries with pulsating stars, chromospherically active stars, systems with strong apsidal motion, double eclipsing binaries, and many other bizarre variables.

REFERENCES

Alard, C., and Lupton, R.H. 1998, *ApJ*, **503**, 325.

Andersen, J. 1991, *The Astronomy and Astrophysics Review*, **3**, 91.

Çakırlı, Ö., Özdarcan, O., and Hoyman, B. 2023, *MNRAS*, **526**, 5987.

Christy, C.T., Jayasinghe, T., Stanek, K.Z., *et al.* 2023, *MNRAS*, **519**, 5271.

Duchêne, G., and Kraus, A. 2013, *Ann. Rev. Astron. and Astrophys.*, **51**, 269.

Dworetsky, M.M. 1983, *MNRAS*, **203**, 917.

Graczyk, D., Soszyński, I., Poleski, R., *et al.* 2011, *Acta Astron.*, **61**, 103.

Kapusta, M., and Mróz, P. 2023, *Acta Astron.*, **73**, 197.

Kim, D.-W., Protopapas, P., Bailer-Jones, C.A.L., *et al.* 2014, *A&A*, **566**, A43.

Mennickent, R.E., Pietrzyński, G., Diaz, M., *et al.* 2003, *A&A*, **399**, L47.

Mowlavi, N., Holl, B., Lecoeur-Taïbi, I., *et al.* 2023, *A&A*, **674**, A16.

Mróz, M., Pietrukowicz, P., Poleski, R., *et al.* 2023, *Acta Astron.*, **73**, 127.

Pawlak, M., Graczyk, D., Soszyński, I., *et al.* 2013, *Acta Astron.*, **63**, 323.

Pawlak, M., Soszyński, I., Udalski, A., *et al.* 2016, *Acta Astron.*, **66**, 421.

Pietrukowicz, P., Mróz, P., Soszyński, I., *et al.* 2013, *Acta Astron.*, **63**, 115.

Pietrzyński, G., Graczyk, D., Gallene, A., *et al.* 2019, *Nature*, **567**, 200.

Poleski, R., Soszyński, I., Udalski, A., *et al.* 2010, *Acta Astron.*, **60**, 179.

Poleski, R. 2014, *PASP*, **126**, 509.

Sana, H., Mink, S.E., de Koter, A., *et al.* 2012, *Science*, **337**, 444.

Savitzky, A., and Golay, M.J.E. 1964, *Analytical Chemistry*, **36**, 1627.

Schwarzenberg-Czerny, A. 1996, *ApJ*, **460**, L107.

Skowron, D.M., Skowron, J., *et al.* 2021, *ApJS*, **252**, 23.

Soszyński, I., Udalski, A., Szymański, M.K,. *et al.* 2016, *Acta Astron.*, **66**, 131.

Szklenár, T., Bódi, A., Tarczay-Nehéz, D., *et al.* 2020, *ApJ*, **897**, L12.

Tylenda, R., Hajduk, M., Kamiński, T., *et al.* 2011, *A&A*, **528**, A114.

Udalski, A., Szymański, M., and Szymański, G. 2015, *Acta Astron.*, **65**, 1.

Udalski, A., Soszynski, I., Szymański, M., *et al.* 1998, *Acta Astron.*, **48**, 563.

Watson, C.L., Henden, A.A., and Price, A. 2006, *Society for Astronomical Sciences 25th Annual Symposium*, **25**, 47.

Woźniak, P.R. 2000, *Acta Astron.*, **50**, 421.

Wrona, M., Ratajczak, M., Kołaczek-Szymański, P.A., *et al.* 2022, *ApJS*, **259**, 16.

Wyrzykowski, L., Udalski, A., Kubiak, M., *et al.* 2003, *Acta Astron.*, **53**, 1.

Wyrzykowski, L., Udalski, A., Kubiak, M., *et al.* 2004, *Acta Astron.*, **54**, 1.

Zasche, P., Wolf, M., and Vraštil, J. 2017, *MNRAS*, **472**, 2241.

Zasche, P., Vokrouhlický, D., *et al.* 2019, *A&A*, **630**, A128.

Zasche, P., Wolf, M., *et al.* 2020, *A&A*, **640**, A33.